2014 IEEE International Conference on Robotics & Automation (ICRA)
Hong Kong Convention and Exhibition Center
May 31 - June 7, 2014. Hong Kong, China

Constrained Manipulation in Unstructured Environment Utilizing Hierarchical Task Specification for Indirect Force Controlled Robots

Ewald Lutscher and Gordon Cheng
Institute for Cognitive Systems (www.ics.ei.tum.de)
Technische Universität München

***Abstract*— In this work, we reformulate our previously developed strategy for operating unknown constrained mechanisms, to fit our new task specification framework for indirect force controlled robots, which we presented recently. The main improvement is a significant reduction of erroneous forces, which is achieved by breaking the manipulation task down into a hierarchical set of subtasks instead of having interfering tasks. The improvement is evaluated by conducting a series of manipulation experiments using the old and new approach and comparing the average erroneous forces.**

I. Motivation

Many approaches for constrained manipulation in unstructured environments focus on modeling the constraint and estimate the model parameters as good as possible, e.g. [1], [2], [3], [4], [5], [6]. Active interaction forces, which are required to move along the constrained trajectory are often not considered and these approaches are limited by the underlying model of the constraint. Also, external sensors like vision or laser scanners are often used, which introduce an additional source of uncertainty and make the complete system often quite complicated.

Approaches which use simple models and rely only on internal sensing (position- and force sensors) often assume orthogonal velocity and force subspaces, neglecting potentially required interaction forces (active forces). Examples of such approaches are [7], [8], [9], where only little active forces are postulated.

In [10] and [11] a desired force has to be predefined, what can be problematic for changing required interaction forces, e.g. for latch mechanisms like a microwave door.

In [12] a compliant manipulator is used to pull open doors and drawers. The control goal is to follow the constraint trajectory with the manipulators end effector without considering the actually applied interaction forces. The compliance is used to compensate for uncertainties. This method is improved by learning the kinematics of the operated mechanism in [13].

Karayiannidis et al. proposed a new velocity controller with force feedback to open revolute and prismatic doors and drawers [14], [15]. While stable execution of the task is proven, the well-known potential risk of contact instability when applying force feedback is not discussed.

This work is supported in part within the DFG excellence initiative research cluster Cognition for Technical Systems - CoTeSys (www.cotesys.org).

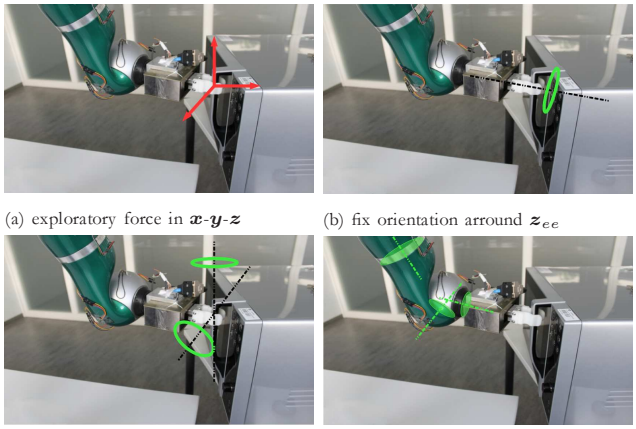

(a) exploratory force in $\boldsymbol{x}$-$\boldsymbol{y}$-$\boldsymbol{z}$ (b) fix orientation arround $\boldsymbol{z}_{ee}$

(c) align $\boldsymbol{z}_{ee}$ with constrained trajectory (d) maximize distance to joint limits

Fig. 1. Breaking down the constrained manipulation task into 4 subtasks

Previously, we proposed a set point generator for indirect force controllers (IFC) in order to operate constrained mechanisms [16]. By using an underlying IFC control scheme, we avoid to design another force controller and instead rely on a well-established and stable control scheme. The major drawback of this approach was, that force and position regulation was realized as two interfering tasks and some gain tuning had to be done to obtain satisfactory results for both tasks.

In [17] we proposed a task specification approach for set point regulation for IFC controlled robots which allowed the independent regulation of static interaction forces and positioning on joint and Cartesian level. The present work shows how to adapt the strategy, developed in [16] for this framework.

The remainder of the paper is structured as follows. Some theoretical basics are recapitulated in section II. In section III, a short review of our previous strategy [16] is given and we show how it can be reformulated for our new framework. The results are presented in IV and a brief summary is given in V.

II. Theoretical Background

A. Manipulator Representation

The very basics of robotic manipulation are assumed to be known, hence only the relations directly in connection to the present work are summarized. The configuration of a manipulator with n degrees of freedom is uniquely determined by a set of n generalized coordinates $\boldsymbol{q}$. For revolute joints $\boldsymbol{q}$ are the joint angles. The end effector pose

can be denoted by a vector $\boldsymbol{x} = [\boldsymbol{p} \quad \boldsymbol{o}]^T$ with the three dimensional position $\boldsymbol{p} = [x\ y\ z]^T$ and orientation $\boldsymbol{o}$, where the dimension and unit of $\boldsymbol{o}$ depend on the chosen orientation representation, e.g. for fixed angles $\boldsymbol{o} = [\phi \quad \theta \quad \psi]^T$, where ϕ, θ and ψ are the rotation angles around the x-, y- and $z-$ axis of the root frame.

For the fixed angle representation, $\dot{\boldsymbol{x}} = [\dot{\boldsymbol{p}} \quad \boldsymbol{\omega}]^T$ denotes the generalized end effector velocity, or twist, with $\dot{\boldsymbol{p}} \in \mathbb{R}^3$ and $\boldsymbol{\omega} \in \mathbb{R}^3$, representing the translational and angular velocity of the end effector. The base Jacobian $\boldsymbol{J}$ states the transformation between joint velocities $\dot{\boldsymbol{q}}$ and the twist:

$$\boldsymbol{J}(\boldsymbol{q}) = \frac{\partial \boldsymbol{x}}{\partial \boldsymbol{q}} = \frac{\dot{\boldsymbol{x}}}{\dot{\boldsymbol{q}}}. \tag{1}$$

Dependencies on $\boldsymbol{q}$ will be omitted for the sake of readability. With (1) the instantaneous inverse kinematics can be inferred using a generalized inverse (e.g. the Moore-Penrose pseudoinverse) of the Jacobian:

$$\dot{\boldsymbol{q}} = \boldsymbol{J}^{+}\dot{\boldsymbol{x}} \tag{2}$$

The transpose of the base Jacobian relates the end effector forces $\boldsymbol{f} \in \mathbb{R}^3$ and moments $\boldsymbol{m} \in \mathbb{R}^3$, to joint torques

$$\boldsymbol{\tau} = \boldsymbol{J}^T\boldsymbol{h},$$

where $\boldsymbol{h} = (\boldsymbol{f} \quad \boldsymbol{m})^T$ is called the end effector wrench. The wrench due to applied torques can be computed vise versa, using a generalized inverse of the transposed base Jacobian.

$$\boldsymbol{h} = \boldsymbol{J}^{T+}\boldsymbol{\tau} \tag{3}$$

B. Indirect Force Control

Indirect force control is characterized by regulating the configuration of a virtual manipulator, represented by its generalized coordinates $\boldsymbol{q}_v$. The relation of this virtual manipulator to the physical manipulator $\boldsymbol{q}$ is stated via a virtual mechanical relationship (see Fig. 2), established either at Cartesian or joint-level. What all joint space IFC schemes have in common, is that they state a virtual stiffness relationship between the position difference $(\boldsymbol{q}_v - \boldsymbol{q})$ and applied joint torque $\boldsymbol{\tau}$ via a stiffness matrix $\boldsymbol{K}$. By determining a set-point $\boldsymbol{q}_v$, the static interaction torque

$$\boldsymbol{\tau} = \boldsymbol{K}(\boldsymbol{q_v} - \boldsymbol{q}) \tag{4}$$

is indirectly induced. A common approach is to use a velocity interface $\dot{\boldsymbol{q}}_v$ to regulate the IFC controlled manipulator.

C. Hierarchical Force and Position Regulation for IFC Controlled Robots

In [17] we generalized m-dimensional force and positioning tasks, using a uniform task variable $\boldsymbol{\sigma} \in \mathbb{R}^m$ with the desired value $\boldsymbol{\sigma}_d$ and

$$\tilde{\boldsymbol{\sigma}}(t) = \boldsymbol{\sigma}_d(t) - \boldsymbol{\sigma}(t)$$

the according task error. The $m \times n$ task Jacobian

$$\boldsymbol{A}_\sigma = \frac{\partial \boldsymbol{\sigma}}{\partial \boldsymbol{q}_v}$$

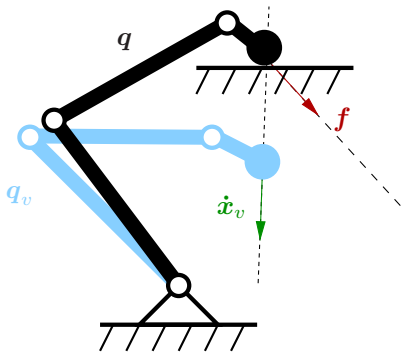

Fig. 2. Motion and interaction forces of the physical manipulator (black) are controlled indirectly by generating set points for the virtual manipulator (blue).

TABLE I
SPECIFICATIONS OF THE FOUR BASIC TASK TYPES

type	$\boldsymbol{\sigma}$	$\boldsymbol{A}_\sigma$
cart. pose	$\boldsymbol{x}_v$	$\boldsymbol{J}_v$
joint position	$\boldsymbol{q}_v$	$\boldsymbol{I}_n$
wrench	$\boldsymbol{h}$	$\boldsymbol{J}^{T+}\boldsymbol{K}$
joint torque	$\boldsymbol{\tau}$	$\boldsymbol{K}$

is defined, giving the linearized relation between $\boldsymbol{\sigma}$ and $\boldsymbol{q}_v$, so that

$$\dot{\boldsymbol{\sigma}} = \boldsymbol{A}_\sigma\dot{\boldsymbol{q}}_v \tag{5}$$

We specified four basic task types, namely

- joint position
- Cartesian end effector pose
- joint torque
- end effector wrench.

With (2), (3) and (4) their task Jacobians can be stated as summarized in table I (see [17] for details). For Cartesian tasks $m = 6$ while for joint space tasks $m = n$. Notice that we consider only the static interaction torques and forces due to the stiffness relation (4). Also, when stating position regulation we are referring to the virtual configuration $\boldsymbol{q}_v$, respectively the Cartesian counterpart $\boldsymbol{x}_v$.

The classical approach for task level control is imposed

$$\dot{\boldsymbol{\sigma}}_d = \boldsymbol{\Lambda}_\sigma\tilde{\boldsymbol{\sigma}}, \tag{6}$$

where $\boldsymbol{\Lambda}_\sigma$ is usually a diagonal, positive definite $m \times m$ gain matrix that tunes the convergence speed of the task error components to $\boldsymbol{0}$. By inverting (5), the general task controller is

$$\dot{\boldsymbol{q}}_{v_d} = \boldsymbol{A}_\sigma^{+}\boldsymbol{\Lambda}_\sigma\tilde{\boldsymbol{\sigma}}, \tag{7}$$

where $\dot{\boldsymbol{q}}_{v_d}$ is the desired velocity of the virtual manipulator. As $\dot{\boldsymbol{q}}_v$ is a virtual quantity, $\dot{\boldsymbol{q}}_{v_d} = \dot{\boldsymbol{q}}_v$ can be assumed.

Every task can be reduced to a certain subspace $\mathbb{S}_\sigma \subseteq \mathbb{R}^m$ which enlarges the manipulators nullspace with respect to that task. This subspace is characterized by a set of

orthonormal vectors, which are the columns of a matrix $\boldsymbol{S}_\sigma$. Therefor the task Jacobian $\boldsymbol{A}_\sigma$ is modified according to

$$\hat{\boldsymbol{A}}_\sigma = \boldsymbol{S}_\sigma^T \boldsymbol{A}_\sigma,$$

which is $\boldsymbol{A}_\sigma$ expressed in $\mathbb{S}_\sigma$.

Having a general task controller (7), a hierarchical controller can be derived using nullspace projection methods to enforce a strict task hierarchy among a set of k subtasks $[\boldsymbol{\sigma}_1 \dots \boldsymbol{\sigma}_k]$. With $\mathrm{Ker}(\boldsymbol{X})$ denoting the orthonormal basis of the kernel of a general linear map $\boldsymbol{X}$, an orthogonal projection operator

$$N(\boldsymbol{X}) = \mathrm{Ker}(\boldsymbol{X})\mathrm{Ker}(\boldsymbol{X})^T$$

is defined, which projects a vector in the nullspace of $\boldsymbol{X}$.

With i as the task iterator and the projector

$$\boldsymbol{N}_i = N([\hat{\boldsymbol{A}}_0 \dots \hat{\boldsymbol{A}}_{i-1}]^T),$$

the k subtasks can be combined in a recursive way by

$$\begin{aligned} \dot{\boldsymbol{q}}_{v_0} &= \boldsymbol{0}, \qquad \hat{\boldsymbol{A}}_0 = \boldsymbol{0}_n \\ \dot{\boldsymbol{q}}_{v_i} &= \dot{\boldsymbol{q}}_{v_{i-1}} + \boldsymbol{N}_i \hat{\boldsymbol{A}}_i^+ (\boldsymbol{\Lambda}_i \tilde{\boldsymbol{\sigma}}_i - \hat{\boldsymbol{A}}_i \dot{\boldsymbol{q}}_{v_{i-1}}), \end{aligned} \tag{8}$$

with $\boldsymbol{0}_n$ as an $n \times n$ matrix with all entries equal to 0.

Having this framework set up, a task can be programmed by specifying a set of subtasks, each defined by a desired task variable $\boldsymbol{\sigma}_d$, the task type, a gain matrix $\boldsymbol{\Lambda}_\sigma$ and a subspace matrix $\boldsymbol{S}_\sigma$.

III. Constrained Manipulation via Hierarchical Task Specification for IFC

In this section we adapt our constraint manipulation strategy from [16] to suit the new task specification approach from [17]. First, the previous strategy is recapitulated, than we show how it can be reformulated in compliance with our new framework by breaking the manipulation task down to a hierarchical set of subtasks (see Fig. 1 for an exemplary task).

A. Review of the Previous Approach

In [16] a first order constraint estimator was used to obtain an estimation for the constraint tangent $\boldsymbol{d}$, what effectively represents the instantaneous desired direction of interaction forces. In the following, when using $\boldsymbol{d}$, we are referring to the estimated value and are not introducing an extra variable for the sake of readability. The constraint was assumed affecting only the translational degrees of freedom, hence $\boldsymbol{d} \in \mathbb{R}^3$ and $||\boldsymbol{d}|| = 1$. An exploratory force along $\boldsymbol{d}$ was induced, by incrementing the joint space set point $\boldsymbol{q}_v$ with a discrete exploration term

$$\boldsymbol{\delta q}_{\mathrm{exp}} = \boldsymbol{K}^{-1} \boldsymbol{J}^T \begin{pmatrix} \kappa \boldsymbol{d} \\ \boldsymbol{0} \end{pmatrix} \Delta T \tag{9}$$

with $\kappa > 0$ as the desired slope of the force along $\boldsymbol{d}$, denoting the rate of the exploration and having the unit N/s. The sampling time of the discrete controller is denoted by ΔT.

To keep the interaction force aligned with $\boldsymbol{d}$, $\boldsymbol{q}_v$ was projected on $\boldsymbol{d}_q = \frac{\boldsymbol{\delta q}_{\mathrm{exp}}}{|\boldsymbol{\delta q}_{\mathrm{exp}}|}$, resulting in the overall set point update

$$\boldsymbol{q}_v[i+1] = \boldsymbol{q}[i] + \boldsymbol{d}_q \boldsymbol{d}_q^T (\boldsymbol{q}_v[i] - \boldsymbol{q}[i]) + \boldsymbol{\delta q}_{\mathrm{exp}}. \tag{10}$$

When using (9) this projection kept the interaction moments equal to zero. To regulate the orientation, a proportional orientation regulator

$$\boldsymbol{\delta q}_\omega = \lambda \boldsymbol{J}^+ \begin{pmatrix} \boldsymbol{0} \\ \tilde{\boldsymbol{o}} \end{pmatrix} \Delta T \tag{11}$$

was imposed and added to (10), with $\tilde{\boldsymbol{o}} = \boldsymbol{o}_d - \boldsymbol{o}_v$ as the orientation error and λ as a constant positive factor, regulating $\tilde{\boldsymbol{o}}$ to $\boldsymbol{0}$.

The major problem with this approach is that (11) is interfering with the main force task pursued by (10). This is resolved by separating the force and positioning task in a hierarchical way, as realized in our task specification framework for indirect force controlled robots ([17]).

B. Constraint Exploration

First, the exploration regulator (10) has to be reformulated as a force task to fit our framework. Hence, the primary task type is end effector wrench, which has to be formulated to keep the exploratory nature of (10). This is achieved by incrementing the currently applied interaction force by the constant $\kappa \Delta T$ along $\boldsymbol{d}$. The according subspace matrix $\boldsymbol{S}_1$ has to reduce the task to the translational degrees of freedom. Hence,

$$\begin{aligned} \boldsymbol{S}_1 &= \begin{bmatrix} \boldsymbol{I}_3 \\ \boldsymbol{0}_3 \end{bmatrix} \\ \boldsymbol{\sigma}_{1_d} &= \boldsymbol{f}_d = \boldsymbol{d}\boldsymbol{d}^T \boldsymbol{f} + \Delta T \ \kappa \boldsymbol{d}, \end{aligned} \tag{12}$$

with $\boldsymbol{I}_3$ being the 3×3 identity matrix. The first term of (12) is the orthogonal projection of the currently applied static interaction forces $\boldsymbol{f} = \boldsymbol{J}^{T+} \boldsymbol{K}(\boldsymbol{q}_v - \boldsymbol{q})$ on the estimated constraint tangent $\boldsymbol{d}$. The second term induces an exploratory force along $\boldsymbol{d}$ with slope κ. A visualization of this action is provided in Fig. 3. This strategy makes sure, that the exerted force automatically adjusts itself to the required interaction force of the operated mechanism while erroneous forces are reduced (see [16] for details).

C. Orientation Regulation

Having the constraint exploration on the top level, regulation of the orientation can be treated in any desired way, since it will be executed in the nullspace of the exploration task. For example, if the end effector is supposed to hold its initial orientation $\boldsymbol{o}_{\mathrm{init}}$, the second task specification would be

$$\begin{aligned} \boldsymbol{S}_2 &= \begin{bmatrix} \boldsymbol{0}_3 \\ \boldsymbol{I}_3 \end{bmatrix} \\ \boldsymbol{\sigma}_{2_d} &= \boldsymbol{o}_{\mathrm{init}}, \end{aligned}$$

with task type Cartesian end effector pose.

Usually the end effector orientation is supposed to adjust itself to the constrained trajectory, e.g. when opening a door,

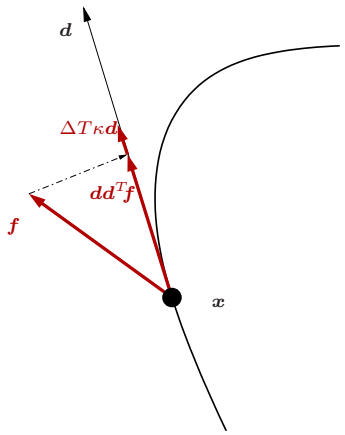

Fig. 3. The currently applied static interaction force $\boldsymbol{f} = \boldsymbol{J}^{T+}\boldsymbol{K}(\boldsymbol{q}_v - \boldsymbol{q})$ is orthogonally projected on the estimated constraint tangent $\boldsymbol{d}$. The exploration term $\Delta T \kappa \boldsymbol{d}$ leads to accumulating forces along $\boldsymbol{d}$.

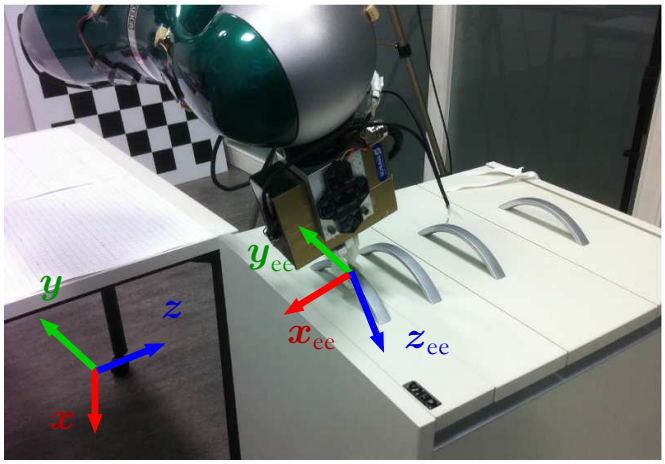

Fig. 4. The experimental setup with end effector and base frame. The drawer has a mass of approximately 1.2 kg, hence requires active interaction forces for successful manipulation.

the z-axis of the end effector ($\boldsymbol{z}_{ee}$) should be aligned with the movement direction. The end effector and base frame of the regarded setup is depicted in Fig.4. Assuming the constraint does not impose a screw motion on the end effector (rotation around $\boldsymbol{z}_{ee}$), the orientation regulation task can be specified to align $\boldsymbol{z}_{ee}$ with the current estimation $\boldsymbol{d}$ using two subtasks:

$$\boldsymbol{S}_2 = \boldsymbol{T}_{IR}[0\ 0\ 0\ 0\ 0\ 1]^T$$
$$\boldsymbol{\sigma}_{2_d} = \boldsymbol{S}_2^T \boldsymbol{x}_{\text{init}}$$

$$\boldsymbol{S}_3 = \boldsymbol{T}_{IR} \begin{bmatrix} 0 & 0 \\ 0 & 0 \\ 0 & 0 \\ 1 & 0 \\ 0 & 1 \\ 0 & 0 \end{bmatrix}$$

$$\dot{\boldsymbol{\sigma}}_{3_d} = \boldsymbol{\Lambda}_3 \boldsymbol{S}_3^T \begin{bmatrix} 0 \\ 0 \\ 0 \\ -\boldsymbol{z}_{ee} \times \boldsymbol{d} \end{bmatrix}$$

With $\boldsymbol{R}_{ee}$ being the end effector rotation matrix, the 6×6 matrix $\boldsymbol{T}_{IR} = \text{diag}(\boldsymbol{I}_3, \boldsymbol{R}_{ee})$ transforms the rotational components of a Cartesian subspace matrix from end-effector to base coordinates. Here, task 2 keeps the orientation around $\boldsymbol{z}_{ee}$ constant, while task 3 aligns $\boldsymbol{z}_{ee}$ with $\boldsymbol{d}$, assuming a pulling task[1]. For convenience, both tasks $\boldsymbol{\sigma}_d$, respectively $\dot{\boldsymbol{\sigma}}_d$ is formulated in base coordinates and then transformed to $\mathbb{S}_\sigma$ using $\boldsymbol{S}_\sigma^T$ for convenience. The two in principle independent orientation tasks are separated nevertheless, as the constant orientation around $\boldsymbol{z}_{ee}$ is more crucial than the orientation around $\boldsymbol{x}_{ee}$ and $\boldsymbol{y}_{ee}$ due to the shape of the end effector[2] and has higher priority in case the orientation subtask can not be fulfilled completely.

Assuming a caging grasp, another possibility for an orientation regulator can be defined, which would permit rotations around $\boldsymbol{y}_{ee}$. This direction could than be used by lower priority tasks. This orientation task would be specified with

$$\boldsymbol{S}_2 = \boldsymbol{T}_{IR}[0\ 0\ 0\ 0\ 0\ 1]^T$$
$$\boldsymbol{\sigma}_{2_d} = \boldsymbol{S}_2^T \boldsymbol{x}_{\text{init}}$$

$$\boldsymbol{S}_3 = \boldsymbol{T}_{IR}[0\ 0\ 0\ 1\ 0\ 0]^T$$
$$\dot{\boldsymbol{\sigma}}_{3_d} = \boldsymbol{\Lambda}_3 \boldsymbol{S}_3^T \begin{bmatrix} 0 \\ 0 \\ 0 \\ -\boldsymbol{z}_{ee} \times \boldsymbol{d} \end{bmatrix}$$

what shifts the rotational degree of freedom around $\boldsymbol{y}_{ee}$ to the nullspace of the manipulator with respect to that task.

D. Remaining Degrees of Freedom

The rest of the manipulators degrees of freedom can be used in order to fulfill any standard manipulation nullspace task. For example, keeping the joints away from their limits (task type: joint position) or minimizing joint torques (task type: joint torques). Suppose, the manipulator kinematics are defined so that $\boldsymbol{q} = \boldsymbol{0}$ denotes the configuration, which maximizes the distance of each joint to its limit, the desired task variable and subspace matrix for both examples would be

$$\boldsymbol{S}_{4(3)} = \boldsymbol{I}_n$$
$$\boldsymbol{\sigma}_{4_d(3_d)} = \boldsymbol{0}.$$

IV. Results

For the experimental evaluation we used our KUKA lightweight arm, running a joint space impedance control. Details on the controller can be found in [18]. The task is lifting a $1.2kg$ mass to a height of $0.3m$, constrained to a linear trajectory (pulling a drawer in vertical direction, see

[1] for pushing, the sign of $\dot{\boldsymbol{\sigma}}_{3_d}$ has to be reversed

[2] In real world applications the used gripper has still some freedom around $\boldsymbol{x}_{ee}$ and $\boldsymbol{y}_{ee}$ due to slippage. A screwing motion (rotation around $\boldsymbol{z}_{ee}$) however would directly induce moments at the end effector and could lead to its damage.

Fig. 4). To compare the previous and our new approach independent from the constraint estimation, we induced a constant estimation ($\boldsymbol{d} = (-1\ 0\ 0)^T$) which corresponds basically to the real direction of motion. However, erroneous forces still appear, especially for faster motions. This is due to unconsidered dynamic effects in combination with a not perfectly rigid constraint (slippage of grasp, play in the drawer mechanism), which lead to a deviation of the end effector from the straight line.

For the new and the old approach, we conducted 9 manipulations with varying stiffness $\boldsymbol{K}$ and varying exploration rate κ. To quantify the increased performance when using the task specification framework compared to our old approach, we compared the root mean square (*RMS*) of the magnitude of the erroneous forces $||\boldsymbol{f}_\perp||$, defined as the passive forces, which are orthogonal to the constraint direction. The effects of different stiffness and exploration rate parameters are discussed in figures 5 and 6. Both show $||\boldsymbol{f}_\perp||$ for two samples of each approach. With the orientation task no longer interfering with the force task, the overall RMS of $||\boldsymbol{f}_\perp||$ for the experiments with fixed estimation $\boldsymbol{d}$, was reduced from $0.58N$ to $0.17N$, which corresponds to a reduction of 70%.

For a more qualitative comparison, we also did 6 trials using the simple velocity filter from [16] as constraint estimator. As expected, we obtained an even higher performance gain, as the reduced erroneous forces lead to a decreased estimation error, what on its part again reduces the erroneous forces. The RMS was reduced from $11.17N$ to $1.54N$, what corresponds to a reduction of 86%.

V. Conclusion

We showed how our previous constrained manipulation strategy could be incorporated in our recently developed task specification framework for indirect force controlled robots. The relative force error is significantly reduced due to the clean separation of the subtasks, what was experimentally evaluated. Besides the usage of a minimal model (constraint tangent), considering active interaction forces and dispense with special hardware devices (e.g. tactile sensors), the main advantage of our approach, is that we do not introduce another control architecture but provide basically an application for the well studied indirect force control scheme, which has proven its robustness for physical interaction tasks.

References

[1] L. Peterson, D. Austin, D. Kragic, and L. Petersson, "High-level control of a mobile manipulator for door opening," in *Proceedings. 2000 IEEE/RSJ International Conference on Intelligent Robots and Systems (IROS 2000) (Cat. No.00CH37113)*. Ieee, 2000, pp. 2333–2338.

[2] C. Rhee, M. Kim, and H. Lee, "Door opening control using the multi-fingered robotic hand for the indoor service robot," in *IEEE International Conference on Robotics and Automation, ICRA*. Ieee, 2004, pp. 4011–4016 Vol.4.

[3] A. Petrovskaya and A. Ng, "Probabilistic Mobile Manipulation in Dynamic Environments, with Application to Opening Doors." in *IJCAI*. Morgan Kaufmann Publishers Inc., 2007, pp. 2178–2184.

[4] J. De Schutter, T. De Laet, J. Rutgeerts, W. Decré, R. Smits, E. Aertbeliën, K. Claes, and H. Bruyninckx, "Constraint-based task specification and estimation for sensor-based robot systems in the presence of geometric uncertainty," *The International Journal of Robotics Research*, vol. 26, no. 5, p. 433, 2007.

[5] W. Meeussen, M. Wise, S. Glaser, S. Chitta, C. McGann, P. Mihelich, E. Marder-Eppstein, M. Muja, V. Eruhimov, T. Foote, and Others, "Autonomous door opening and plugging in with a personal robot," in *International Conference on Robotics and Automation (ICRA), 2010 IEEE*. IEEE, 2010, pp. 729–736.

[6] T. Ruhr, J. Sturm, and D. Pangercic, "A generalized framework for opening doors and drawers in kitchen environments," in *IEEE International Conference on Robotics and Automation*, 2012, pp. 3852–3858.

[7] A. Schmid, N. Gorges, D. Goger, and H. Worn, "Opening a Door with a Humanoid Robot Using Multi-Sensory Tactile Feedback," in *Robotics and Automation, 2008. ICRA 2008. IEEE International Conference on*. IEEE, 2008, pp. 285–291.

[8] W. Chung, C. Rhee, Y. Shim, H. Lee, and S. Park, "Door-Opening Control of a Service Robot Using the Multifingered Robot Hand," *IEEE Transactions on Industrial Electronics*, vol. 56, no. 10, pp. 3975–3984, Oct. 2009.

[9] D. Ma, H. Wang, and W. Chen, "Unknown constrained mechanisms operation based on dynamic hybrid compliance control," in *2011 IEEE International Conference on Robotics and Biomimetics*. Ieee, Dec. 2011, pp. 2366–2371.

[10] G. Niemeyer and J. Slotine, "A simple strategy for opening an unknown door," in *Robotics and Automation, 1997. Proceedings., 1997 IEEE International Conference on*, vol. 2, no. April. IEEE, 1997, pp. 1448–1453.

[11] M. Prats, S. Wieland, T. Asfour, A. del Pobil, and R. Dillmann, "Compliant interaction in household environments by the Armar-III humanoid robot," in *8th IEEE-RAS International Conference on Humanoid Robots*, 2008, pp. 475–480.

[12] A. Jain and C. C. Kemp, "Pulling open novel doors and drawers with equilibrium point control," in *2009 9th IEEE-RAS International Conference on Humanoid Robots*. Ieee, Dec. 2009, pp. 498–505.

[13] J. Sturm, A. Jain, and C. Stachniss, "Operating articulated objects based on experience," in *IEEE/RSJ International Conference on Intelligent Robots and System*, 2010, pp. 2739–2744.

[14] Y. Karayiannidis and C. Smith, "Open Sesame! Adaptive Force/Velocity Control for Opening Unknown Doors," in *IEEE/RSJ International Conference on Intelligent Robots and System*, 2012, pp. 4040–4047.

[15] Y. Karayiannidis, C. Smith, F. Vina, P. Ogren, and D. Kragic, "Model-free robot manipulation of doors and drawers by means of fixed-grasps," in *IEEE International Conference on Robotics and Automation*, 2013, pp. 4470–4477.

[16] E. Lutscher and G. Cheng, "A set-point-generator for indirect-force-controlled manipulators operating unknown constrained mechanisms," in *2012 IEEE/RSJ International Conference on Intelligent Robots and Systems*. Ieee, Oct. 2012, pp. 4072–4077.

[17] ——, "A Practical Approach to Generalized Hierarchical Task Specification for Indirect Force Controlled Robots," in *IEEE/RSJ International Conference on Intelligent Robots and System*, 2013.

[18] A. Albu-Schäffer, C. Ott, and G. Hirzinger, "A unified passivity based control framework for position, torque and impedance control of flexible joint robots," *Robotics Research*, pp. 5–21, 2007.

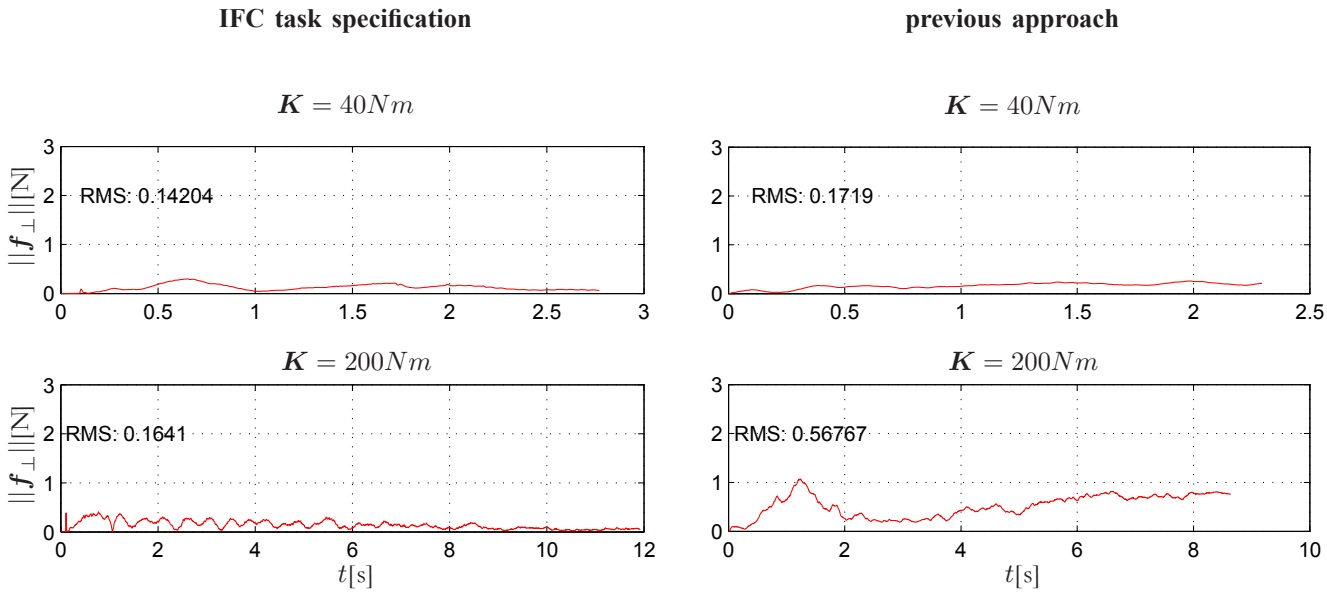

Fig. 5. Pulling the drawer with fixed exploration speed $\kappa = 10\frac{N}{s}$ and varying stiffness $\boldsymbol{K}$. Left: utilizing our new task specification scheme for IFC controlled robots. Right: previous approach with conflicting subtasks. For high compliance ($\boldsymbol{K} = 40Nm$), the two approaches perform almost equal, as the positioning task has only minor impact on the force task. With a stiffer manipulator ($\boldsymbol{K} = 200Nm$), the sensitivity of the force task to the positioning task is higher, what leads to increased erroneous forces when using our previous approach. The higher stiffness results also in a higher execution time, as the motion speed is reduced due to the higher sensitivity of the force task to $\dot{\boldsymbol{q}}_v$.

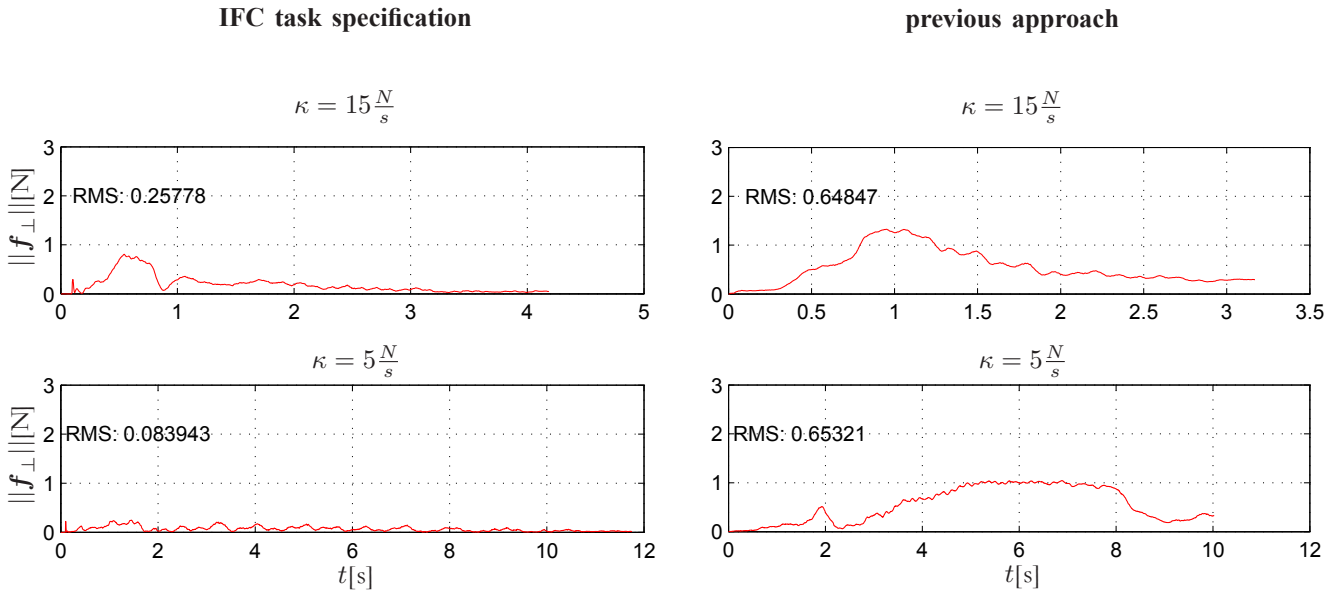

Fig. 6. Pulling the drawer with fixed stiffness $\boldsymbol{K} = 100Nm$ and varying exploration rate κ. Left: utilizing our new task specification scheme for IFC controlled robots. Right: previous approach with conflicting subtasks. The improved performance of the new approach is apparent for lower exploration rates ($\kappa = 5\frac{N}{s}$), as dynamic effects are almost not existent and the new task specification framework generates effectively no erroneous forces. With a higher exploration rate ($\kappa = 15\frac{N}{s}$) also the effective erroneous forces rise slightly, especially in the beginning, where acceleration is higher. For the previous approach, the induced erroneous forces due to conflicting subtasks are dominating and are not noticeably increased by a higher exploration rate.